

## Paper

# Performance and operation of stressed dual gap RF MEMS varactors

Greg McFeetors and Michal Okoniewski

**Abstract**— The design, fabrication and measurement of a continuously tunable RF MEMS capacitor is described. The capacitor's dual gap height architecture allows for electrostatic tuning with low resistive loss and a large tuning range. A new dual tuning scheme is introduced for use with two voltage sources. This dual tuning, coupled with a stress-induced bridge, is used to reach further device tuning. Measurements indicate a continuously tunable capacitance range of 6.2:1 with a quality factor over 50 at 30 GHz for 310 fF.

**Keywords**— *electromechanical systems (MEMS), varactors, capacitors, Q factor.*

## 1. Introduction

Microelectromechanical systems (MEMS) have demonstrated excellent characteristics as microwave circuit components. In particular, switches and capacitors have proven to have excellent radio frequency (RF) specifications due to the low loss and inherent mechanical tunability of MEMS structures [1]. While most MEMS variable capacitors reported have been developed as digitally-switched capacitors, continuously tunable capacitors are often beneficial where high tuning range is required. Analog MEMS varactors can possibly offer an integration-friendly, low-loss replacement for diode varactors, however, until recently, MEMS varactors have suffered from poorer tuning range than their diode counterparts.

Quite recently, a number of RF MEMS varactors have been designed and fabricated for use at RF with excellent quality factors at frequencies up to 40 GHz. A summary of recently reported analog MEMS varactors is shown in Table 1, along with the results of this work. As quality factor is dependant on frequency and capacitance, the notable metric columns are tuning range and equivalent series resistance (ESR).

Table 1  
High-Q RF MEMS varactor comparison

Device	Frequency [GHz]	Q	Tuning	Value	ESR [ $\Omega$ ]
Dusopt [2]	34	95	1.5:1	80 fF	0.6
Borwick [3]	3	25	8.4:1	1.5 pF	1.42
Chen [4]	5	30	1.7:1	60 fF	17
Dec [5]	1	20	1.87:1	2.05 pF	3
Peroulis [6]	40	80	3:1	168 fF	0.3
This work	30	52	6.2:1	310 fF	0.34

## 2. Design

Electrostatic actuation of MEMS beams is easily amenable to a tunable parallel plate capacitor design. While both cantilever (single-fixed) and bridge (fixed-fixed) beam designs have been utilized for MEMS capacitors, the bridge design presents higher stable continuous tuning in its simplest form [7] and is used as a basis for this work.

The stable continuous tuning range is limited in all simple electrostatic beam actuator designs. A flat, fixed beam, with force applied at the center can only obtain a continuous tuning range of 1.5:1, or 50%, before pull-in. However, electrode placement can effect the pull-in deflection, both by increasing the “beam stretching” [8] and using “beam leveraging” [9]. This is done by placing the bottom DC electrodes at the ends of the beam, rather than the center. This alteration can increase the deflection at the beam center to beyond 50% of the initial beam height.

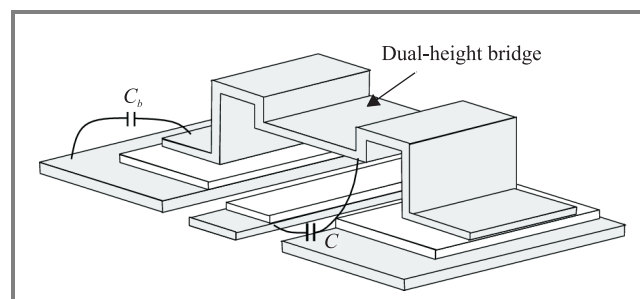
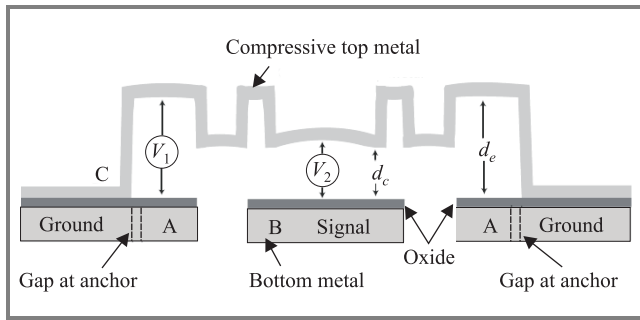


Fig. 1. Planar MEMS bridge geometry isometric view.

A method for greater tuning has been implemented by the authors in [10] using a two-layered bridge with dual gap heights, shown in Fig. 1. This architecture avoids the pull-in limitation by separating the capacitance plate gap ( $d_c$ ) from the electrostatic electrode gap ( $d_e$ ), as shown in Fig. 2. Therefore, the pull-in deflection at the electrodes corresponds to the larger deflection ratio at the capacitor. Electrostatic electrodes at the ends of the beam also create the leveraging and stretching effects. However, the tuning of this device is still limited to 4:1 due to the compressive beam stress and beam curvature under deflection, as discussed in Section 3.

This has led to a dual-tuning concept, which removes much of the tuning limitation caused by the beam stress and non-planarity, and in fact takes advantage of beam stress to increase tuning range. The device, as fabricated, is shown in Fig. 2. This figure also shows the adaptation of this design to a coplanar waveguide shunt-ground configuration variable capacitor. The signal conductor forms the bottom



**Fig. 2.** High tuning dual-height stressed bridge capacitor profile.

plate of the capacitor, while the ground conductors are used as the bottom electrodes for electrostatic actuation.

Actuation is controlled in two stages: the first stage is controlled by applying a DC voltage from electrodes A to C, with a common voltage on B and C to avoid attraction between these electrodes. The second stage then additionally adds potential difference between electrodes B and C to fully tune the device. Chrome silicide resistive lines can be used to connect DC voltages to B and C, as they supply RF isolation. A thin layer of oxide is used to insulate the top and bottom electrodes, as well as create an RF short,  $C_b$ , between the large top metal anchors and the bottom ground conductor. The design of the capacitor must ensure that the outer electrode length, oxide height, and bridge gap heights are such that the bridge deflection allows for full tuning and bridge center contact before pull-in. These design details are verified using an electromechanical simulator, as discussed in the following section. Furthermore, this design allows for secondary tuning, as also discussed more fully in Section 3.

As shown in Fig. 2, reliability is increased by introducing a small gap in the bottom A electrode at the bridge anchor. This removes the attractive force at the anchor and decreases the bridge deflection at the anchor corner, preventing the bridge from weakening or failing after repeated cycles.

### 3. Modeling and simulation

Dynamic 3D modeling of the MEMS device is performed using the commercial software Coventorware. This allows for simulation of the mechanical and electrical properties of MEMS structures based on the stress, load, and electrostatic forces. Based on the device layout and the measured stress of the thin films, the movement of the bridge can be predicted for various actuation voltages. The geometry of the device and the bridge stress has warranted the need for software simulation of the varactor operation, as closed-form equation modeling has proven inaccurate.

Figure 3 shows the bridge geometry and deflections for 0 V, 30 V, 40 V and 50 V cases. For illustrative purposes, the z-dimension has been scaled by a factor of 10. In this figure, conductor A is grounded, while voltage is applied to conductors B and C (with RF isolation between them).

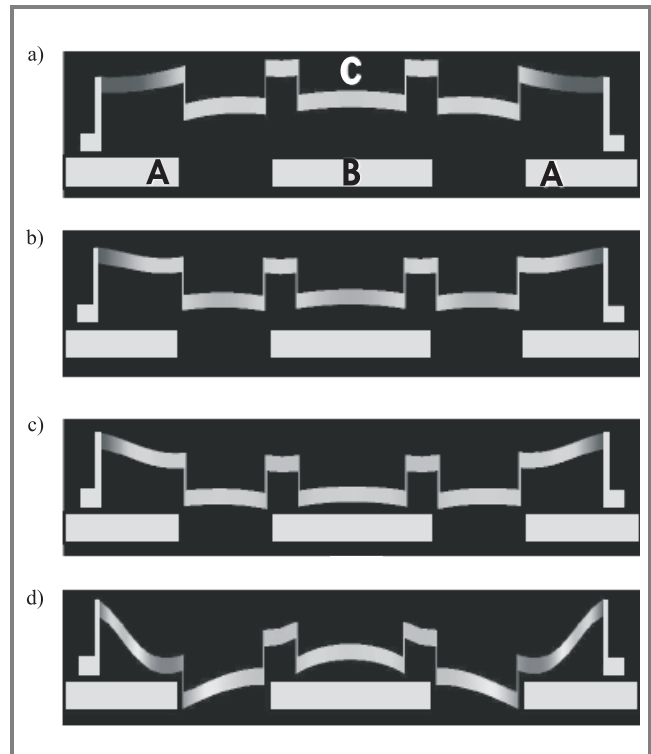


**Fig. 3.** Stage 1 tuning: (a)  $V_{AC} = 0$  V; (b)  $V_{AC} = 30$  V; (c)  $V_{AC} = 40$  V; (d)  $V_{AC} = 50$  V. For all cases  $V_{BC} = 0$  V.

The 30 V case shows mid-range tuning of the device. The 40 V case shows the point at which the bridge comes in contact with the oxide layer. Increasing the voltage further causes the bridge to reach pull-in, as seen by the 50 V case. Interestingly, this causes the beam to lift off the bottom center plate in the middle, due to the intrinsic beam stress and the force caused by the outer electrodes, and hence lowers the capacitance.

The primary continuous tuning range of the capacitor in this configuration is exhausted by varying the voltage on the outer electrodes from 0 V to 40 V. The beam curvature due to stress and deflection curls the top electrode to prevent further tuning, as shown in Figs. 3c and 3d. Thus, a new dual-tuning scheme is then introduced by applying

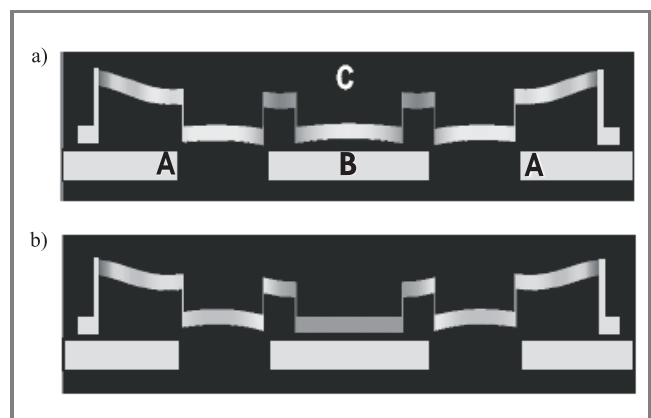


**Fig. 4.** Stage 2 tuning: (a)  $V_{CB} = 10$  V; (b)  $V_{CB} = 25$  V. For both cases  $V_{AC} = 40$  V.

additional voltage between electrodes B and C, which pulls the bridge into the bottom capacitor plate, shown by Fig. 4. The deformation of the bridge due to the outer electrodes produces a nonlinear spring restoration force, allowing the bridge to be significantly flattened before final pull-in.

This two-stage bridge deflection allows for a large tuning range from a relatively simple capacitor structure. Also note that the tuning range of the first stage can be further increased by enlarging the gap height,  $d_e$ , at the consequence of increased actuation voltage.

## 4. Fabrication

The fabrication process used in this project is a modified custom process previously developed by the authors for the fabrication of MEMS RF phase-shifters [10]. The devices are built on a fused silica substrate using surface micromachining. Copper, with its high bulk conductivity, is ideal for forming base conductors of a CPW layer and is deposited, along with titanium adhesion layers and a gold oxidation barrier, using DC magnetron sputtering. The copper lines are then covered in 300 nm of PECVD oxide that serves two purposes: it insulates the signal conductors from the bridge, thus preventing a short-circuit at full bridge deflection, and creates a dielectric layer for a large capacitance between the ground lines and the bridge anchor ( $C_b$ ). This oxide must be carefully processed to avoid dielectric breakdown during actuation. Optional  $\text{CrSi}_2$  resistive lines can then be deposited and patterned, using a sputtering lift-off process.

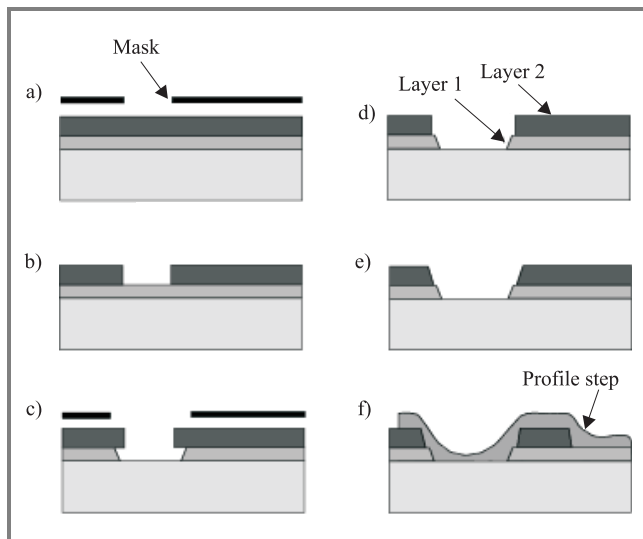


**Fig. 5.** Dual sacrificial layer height process: (a) expose top resist; (b) develop top resist; (c) develop bottom resist and expose top resist; (d) develop top resist; (e) develop sidewalls of top resist; (f) deposit and pattern metal beam.

The bridge requires micromachining with two consecutive sacrificial layers to obtain two different heights. The resulting bridge has a height of 950 nm over the center electrode and oxide, and  $2.5\ \mu\text{m}$  over the side electrodes and oxide.

This unique process, as shown in Fig. 5, is critical to obtain varactors with desirable tuning characteristics.

Aluminum is then deposited at low temperature and low stress ( $< 50\ \text{MPa}$ ) to form the bridge metal. Figure 6 is an SEM picture of a single gap height bridge, demonstrating the near-planar low compressive stress deposition

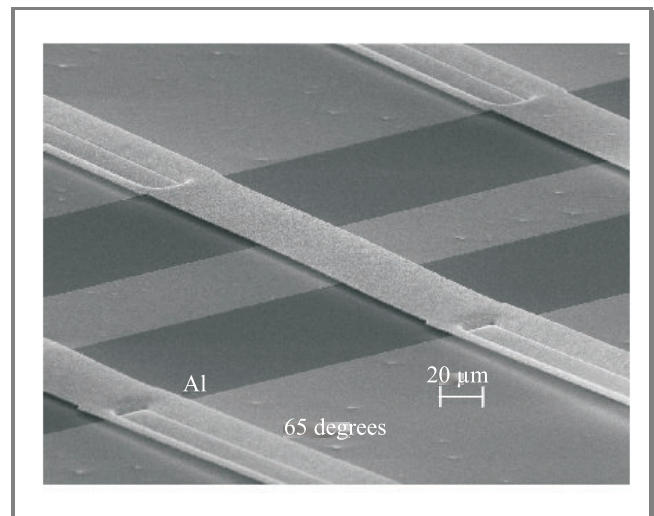


**Fig. 6.** SEM photograph of planar bridge.

technique. To increase the limits of elastic deformation, molybdenum or copper is alloyed with the aluminum to increase the hardness of the metal, minimizing the bridge damage due to plastic deformations. The stress of this film can then be manipulated by controlling the deposition vacuum and temperature, sputtering power, and post-deposition annealing time and temperature. To complete the device, the bridge is released and the structure is critically dried. The final released structure is shown in Fig. 7.

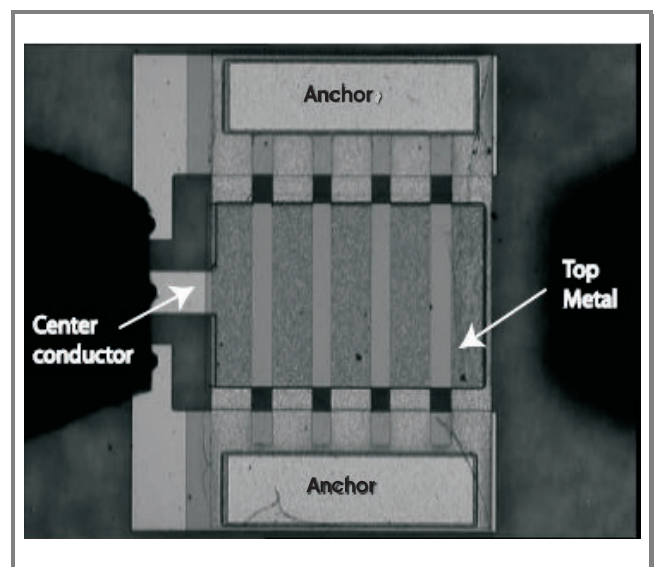


**Fig. 7.** Optical photograph of fabricated capacitor.

An alternative bridge material using electroplated copper has also been fabricated. Near zero stress is possible us-

ing this deposition method ( $< 10$  MPa tensile), allowing for measurement comparison to the aluminum-molybdenum bridges.

All fabrication work was performed by the authors at the Advanced Microfabrication Integration Facility (AMIF) at the University of Calgary and at the Nanofab facility at the University of Alberta.

## 5. Measurements

Measurements have been performed using an E8364A Agilent precision network analyzer (PNA) with the capacitors in shunt-ground configuration. Due to the tolerances of this equipment at lower frequencies and small capacitances,  $Q$  values approaching and greater than 100 cannot be determined with sufficient accuracy. The result of the measurements of the capacitance versus tuning voltage is shown in Fig. 8. The capacitance at 0 V is 310 fF, while 45 V gives 1.4 pF. Utilization of the second tuning stage increases the capacitance to 1.93 pF by changing voltage  $B$  by 25 V, to either 20 V or 70 V.

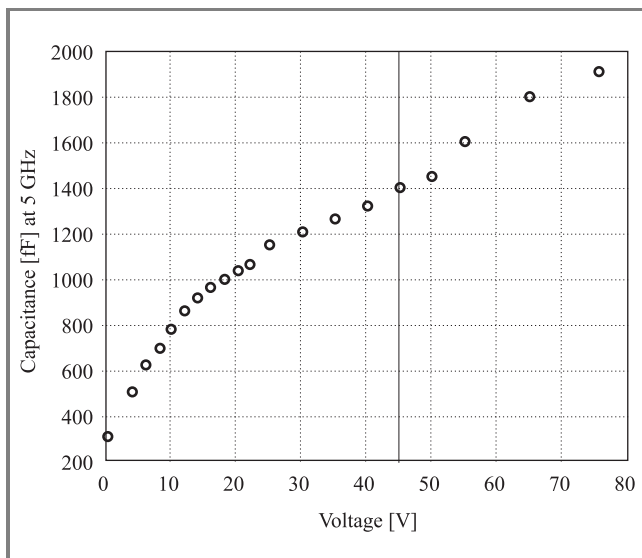


Fig. 8. Capacitance versus voltage with two tuning stages.

This shows a 4.5:1 tuning range using the 1st tuning stage, and 6.2:1 total continuous and repeatable tuning range. The 0 V case gives  $C = 310$  fF and  $Q = 50$  and the 45 V case gives  $C = 1.4$  pF and  $Q = 10.6$  at 30 GHz. This corresponds to  $ESR = 0.34 \Omega$  at 30 GHz for 0 V, and  $0.36 \Omega$  at a 45 V deflection potential.

This two-stage tuning demonstrates an additional 37% device capacitance tuning in the second tuning stage. To demonstrate the dependence on bridge compressive stress, these measurements were compared to near zero-stress bridges of electroplated copper. The electroplated copper devices showed similar tuning in the first stage, however, only an additional 7% tuning could be achieved in the second tuning stage.

## 6. Conclusion

The successful design and custom fabrication of a high tuning RF MEMS varactor utilizing a relatively simple structure has been described. Simulations have also been presented to explain the mechanical properties of the device. Measurements of this device indicate a quality factor of 50 at 30 GHz, with an ESR below  $0.4 \Omega$  and large continuous analog tuning range of 6.2:1 (Fig. 9). To our knowledge, this demonstrates the largest tuning range of any sub- $1 \Omega$  ESR varactor reported to date.

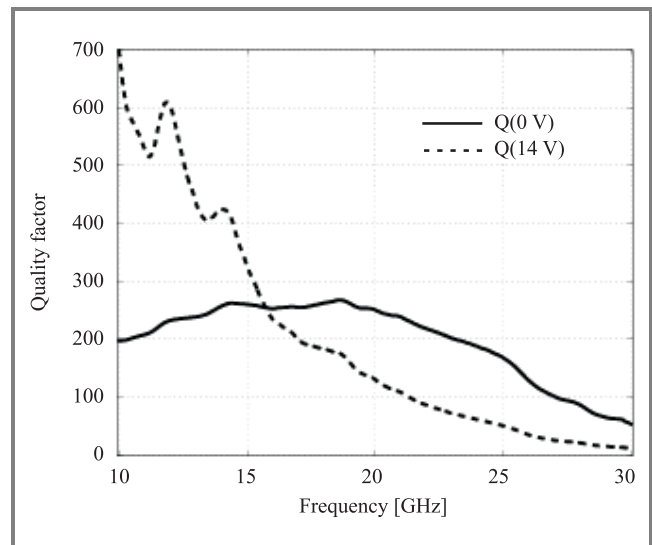


Fig. 9.  $Q$ -factor measurements.

This varactor may be useful in any application where a low loss, large tuning varactor is required. Especially where large resolution tuning is required, analog MEMS varactors may be preferable to digitally switched MEMS variable capacitors, as digital capacitor network can quickly become large and lossy when high capacitance resolution is required. Specifically, this varactor is suitable for applications such as voltage controlled oscillators, phase shifters [10], phased array and tunable reflect-array antennas [11], and high- $Q$  filters.

## Acknowledgment

The authors wish to acknowledge the assistance and support of the National Science and Engineering Research Council of Canada, the Alberta Ingenuity Fund and TR-Labs Calgary.

## References

- [1] S. Lucyszyn, "Review of radio frequency microelectromechanical systems technology", *IEE Proc. Sci. Meas. Technol.*, vol. 151, no. 2, pp. 93–103, 2004.
- [2] L. Dussopt and G. Rebeiz, "High- $Q$  millimeter-wave MEMS varactors: extended tuning range and discrete-position designs", in *IEEE MTT-S Int. Microw. Symp. Dig.*, Seattle, USA, 2002, pp. 1205–1208.



- [3] R. L. Borwick *et al.*, "A high Q large tuning range MEMS capacitor for RF filter systems", *Sens. Actuat. A: Phys.*, vol. 103, no. 1, pp. 33–41, 2003.
- [4] J. Chen *et al.*, "Design and modeling of a micromachined high-Q tunable capacitor with large tuning range and a vertical planar spiral inductor", *IEEE Trans. Electron Dev.*, vol. 30, no. 3, pp. 730–739, 2003.
- [5] A. Dec and K. Suyama, "Micromachined varactors with wide tuning range", *IEEE Trans. Microw. Theory Techn.*, vol. 46, pp. 2587–2596, 1998.
- [6] D. Peroulis, S. Mohammadi, and L. P. B. Katehi, "Electrostatically-tunable analog RF MEMS varactors with measured capacitance range of 300%", in *IEEE MTT-S Int. Microw. Symp. Dig.*, Philadelphia, USA, 2003, vol. 3, pp. 1793–1796.
- [7] G. M. Rebeiz, *RF MEMS Theory, Design, and Technology*. Hoboken: Wiley, 2003.
- [8] E. K. Chan *et al.*, "Design and fabrication of a novel two-dimension MEMS-based tunable capacitor", *IEEE Int. Conf. Commun., Circ. Syst.*, Chengdu, China, 2002, vol. 2, pp. 1766–1769.
- [9] E. S. Hung and S. D. Senturia, "Extending the travel range of analog-tuned electrostatic actuators", *J. Micromech. Syst.*, vol. 8, no. 8, pp. 497–505, 1999.
- [10] G. McFeetors and M. Okoniewski, "Distributed MEMS analog phase shifter with enhanced tuning", *IEEE Microw. Wirel. Compon. Lett.*, vol. 16, no. 1, pp. 34–36, 2006.
- [11] S. V. Hum, G. McFeetors, and M. Okoniewski, "Integrated MEMS reflectarray elements", in *1st Eur. Conf. Anten. Propagat.*, Nice, France, 2006.



**Greg McFeetors** received the B.Sc. degree from the University of Manitoba and the M.Sc. degree from the University of Calgary in 2000 and 2004, respectively. He is currently a Ph.D. student at the University of Calgary. His current research interests lie in RF MEMS systems design, fabrication, and applications, including

varactors, inductors, antenna systems, filters, and various applications of MEMS into communications circuits. He is also affiliated with TR-Labs Calgary.

e-mail: geomcfee@ucalgary.ca

Department of Electrical and Computer Engineering  
University of Calgary

2500 University Drive N.W.

Calgary, Alberta, T2J 1K5, Canada



**Michal Okoniewski** is a Professor and Canada Research Chair with the Department of Electrical and Computer Engineering, University of Calgary. He is also affiliated with TR-Labs Calgary. Doctor Okoniewski received the M.Sc. and Ph.D. degrees from the Gdańsk University of Technology, Poland. He is a Senior

Member of IEEE, Associate Editor for "IEEE Transactions on Antennas and Propagation" and member of IEEE Standard Groups. Doctor Okoniewski is interested in many aspects of applied electromagnetics, ranging from computational electrodynamics, to reflectarrays and self configuring antennas, RF MEMS, and re-configurable computational hardware for electromagnetics applications. He is also actively involved in bio-electromagnetics, where he works on tissue spectroscopy and cancer detection.

e-mail: michal@enel.ucalgary.ca

Department of Electrical and Computer Engineering  
University of Calgary

2500 University Drive N.W.

Calgary, Alberta, T2J 1K5, Canada